

000 054  
 001 055  
 002 056  
 003 057  
 004 058  
 005 059  
 006 060  
 007 061  
 008 062  
 009 063  
 010 064  
 011 065  
 012 066  
 013 067  
 014 068  
 015 069  
 016 070  
 017 071  
 018 072  
 019 073  
 020 074  
 021 075  
 022 076  
 023 077  
 024 078  
 025 079  
 026 080  
 027 081  
 028 082  
 029 083  
 030 084  
 031 085  
 032 086  
 033 087  
 034 088  
 035 089  
 036 090  
 037 091  
 038 092  
 039 093  
 040 094  
 041 095  
 042 096  
 043 097  
 044 098  
 045 099  
 046 100  
 047 101  
 048 102  
 049 103  
 050 104  
 051 105  
 052 106  
 053 107

## Supplementary Material to “External Prior Guided Internal Prior Learning for Real Noisy Image Denoising”

Anonymous CVPR submission

Paper ID 1047

In this supplementary material, we provide:

1. The closed-form solution of the proposed weighted sparse coding model in the main paper.
2. More denoising results on the real noisy images (with no “ground truth”) provided in the dataset [1].
3. More denoising results on the 15 cropped real noisy images (with “ground truth”) used in the dataset [2].
4. More denoising results on the 60 cropped real noisy images (with “ground truth”) from [2].

### 1. Closed-Form Solution of the Weighted Sparse Coding Problem (4)

The weighted sparse coding problem in the main paper is:

$$\min_{\alpha} \|\mathbf{y} - \mathbf{D}\alpha\|_2^2 + \|\mathbf{w}^T \alpha\|_1. \quad (1)$$

Since  $\mathbf{D}$  is an orthonormal matrix, problem (1) is equivalent to

$$\min_{\alpha} \|\mathbf{D}^T \mathbf{y} - \alpha\|_2^2 + \|\mathbf{w}^T \alpha\|_1. \quad (2)$$

For simplicity, we denote  $\mathbf{z} = \mathbf{D}^T \mathbf{y}$ . Since  $\mathbf{w}_i = c * 2\sqrt{2}\sigma^2 / (\Lambda_i + \varepsilon)$  is positive (please refer to Eq. (18) in the main paper), problem (2) can be written as

$$\min_{\alpha} \sum_{i=1}^{p^2} ((\mathbf{z}_i - \alpha_i)^2 + \mathbf{w}_i |\alpha_i|). \quad (3)$$

The problem (3) is separable w.r.t.  $\alpha_i$  and can be simplified to  $p^2$  scalar minimization problems

$$\min_{\alpha_i} (\mathbf{z}_i - \alpha_i)^2 + \mathbf{w}_i |\alpha_i|, \quad (4)$$

where  $i = 1, \dots, p^2$ . Taking derivative of  $\alpha_i$  in problem (4) and setting the derivative to be zero. There are two cases for the solution.

(a) If  $\alpha_i \geq 0$ , we have

$$2(\alpha_i - \mathbf{z}_i) + \mathbf{w}_i = 0. \quad (5)$$

The solution is

$$\hat{\alpha}_i = \mathbf{z}_i - \frac{\mathbf{w}_i}{2} \geq 0. \quad (6)$$

So  $\mathbf{z}_i \geq \frac{\mathbf{w}_i}{2} > 0$ , and the solution  $\hat{\alpha}_i$  can be written as

$$\hat{\alpha}_i = \text{sgn}(\mathbf{z}_i) * (|\mathbf{z}_i| - \frac{\mathbf{w}_i}{2}), \quad (7)$$

where  $\text{sgn}(\bullet)$  is the sign function.

(b) If  $\alpha_i < 0$ , we have

$$2(\alpha_i - \mathbf{z}_i) - \mathbf{w}_i = 0. \quad (8)$$

The solution is

$$\hat{\alpha}_i = \mathbf{z}_i + \frac{\mathbf{w}_i}{2} < 0. \quad (9)$$

So  $\mathbf{z}_i < -\frac{\mathbf{w}_i}{2} < 0$ , and the solution  $\hat{\alpha}_i$  can be written as

$$\hat{\alpha}_i = \text{sgn}(\mathbf{z}_i) * (-\mathbf{z}_i - \frac{\mathbf{w}_i}{2}) = \text{sgn}(\mathbf{z}_i) * (|\mathbf{z}_i| - \frac{\mathbf{w}_i}{2}). \quad (10)$$

108 In summary, we have the final solution of the weighted sparse coding problem (1) as 162  
 109  $\hat{\alpha} = \text{sgn}(\mathbf{D}^T \mathbf{y}) \odot \max(|\mathbf{D}^T \mathbf{y}| - \mathbf{w}/2, 0),$  163  
 110 where  $\odot$  means element-wise multiplication and  $|\mathbf{D}^T \mathbf{y}|$  is the absolute value of each entry of the vector  $\mathbf{D}^T \mathbf{y}.$  164  
 111  
 112 **2. More Results on Real Noisy Images in [1]** 165  
 113  
 114 In this section, we give more visual comparisons of the competing methods on the real noisy images provided in [1]. The 166  
 115 real noisy images in this dataset [1] have no “ground truth” images and hence we only compare the visual quality of the 167  
 116 denoised images by different methods. As can be seen from Figures 1-4, our proposed method performs better than the state- 168  
 117-of-the-art denoising methods. This validates the effectiveness of our proposed external prior guided internal prior learning 169  
 118 framework for real noisy image denoising. 170  
 119  
 120  
 121  
 122  
 123  
 124  
 125  
 126  
 127  
 128  
 129  
 130  
 131  
 132  
 133  
 134  
 135  
 136  
 137  
 138  
 139  
 140  
 141  
 142  
 143  
 144  
 145  
 146  
 147  
 148  
 149  
 150  
 151  
 152  
 153  
 154  
 155  
 156  
 157  
 158  
 159  
 160  
 161

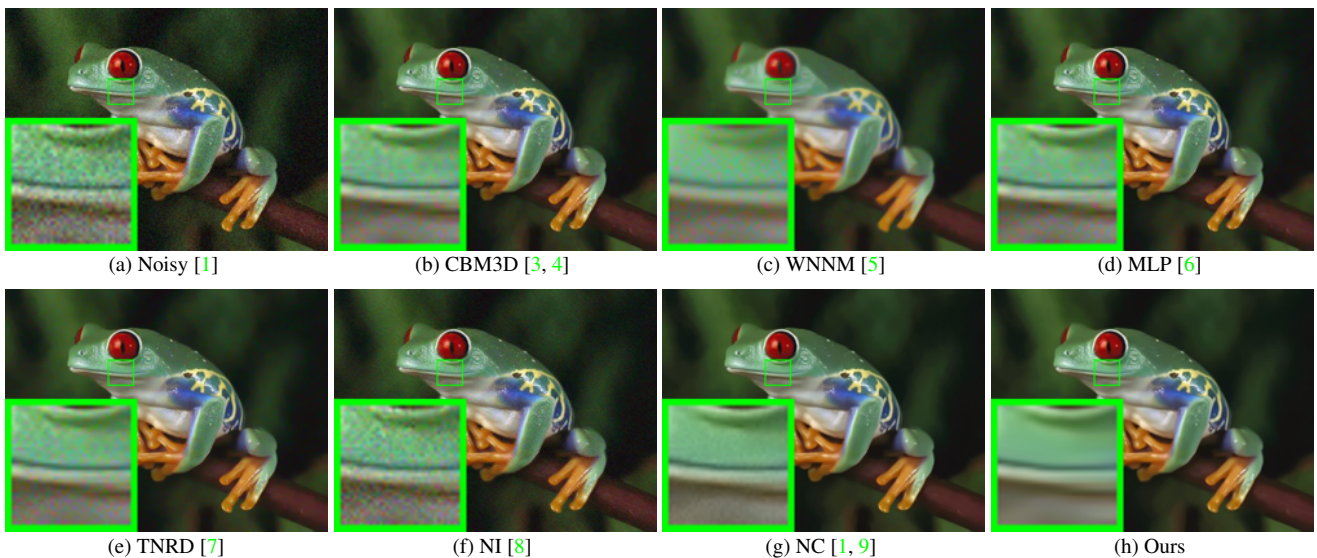


Figure 1. Denoised images of the real noisy image “Frog” [1] by different methods. The images are better to be zoomed in on screen.

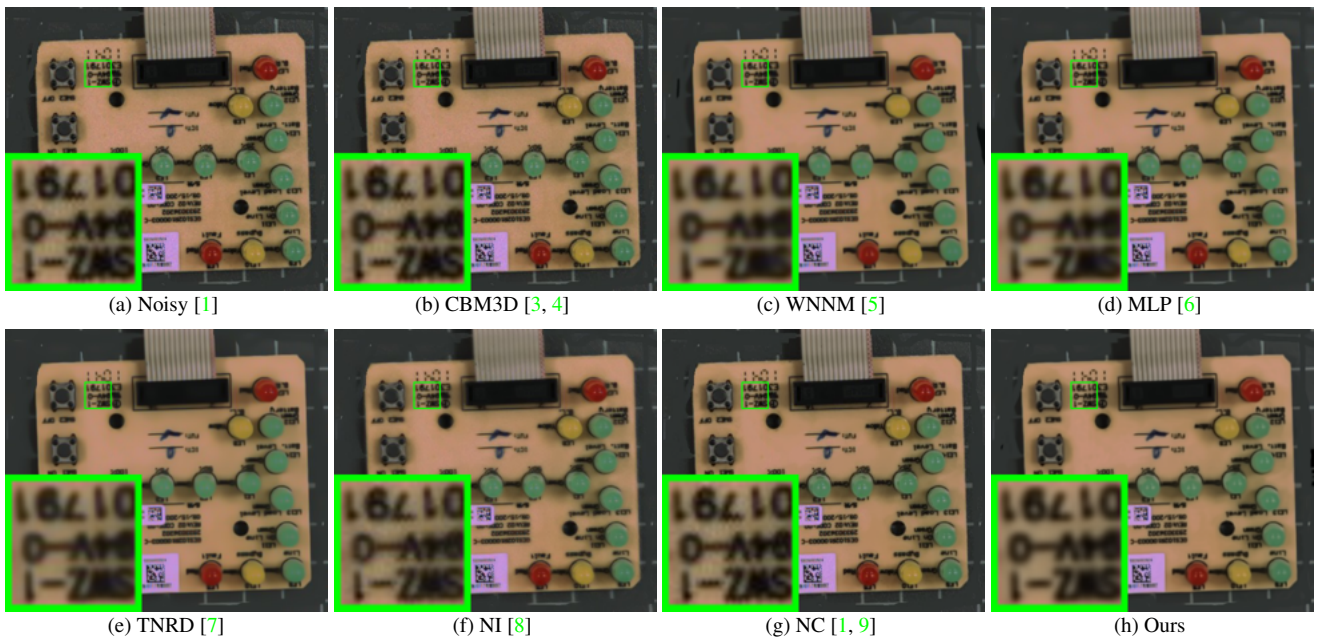


Figure 2. Denoised images of the real noisy image “Circuit” [1] by different methods. The images are better to be zoomed in on screen.

216  
217  
218  
219  
220  
221  
222  
223  
224  
225  
226

(a) Noisy [1] (b) CBM3D [3, 4] (c) WNNM [5] (d) MLP [6]

(e) TNRD [7] (f) NI [8] (g) NC [1, 9] (h) Ours

Figure 3. Denoised images of the real noisy image “Woman” [1] by different methods. The images are better to be zoomed in on screen.

236

237

238

239

240

241

242

243

244

245

246

247

248

249

250

251

252

253

254

255

256

257

258

259

260

261

262

263

264

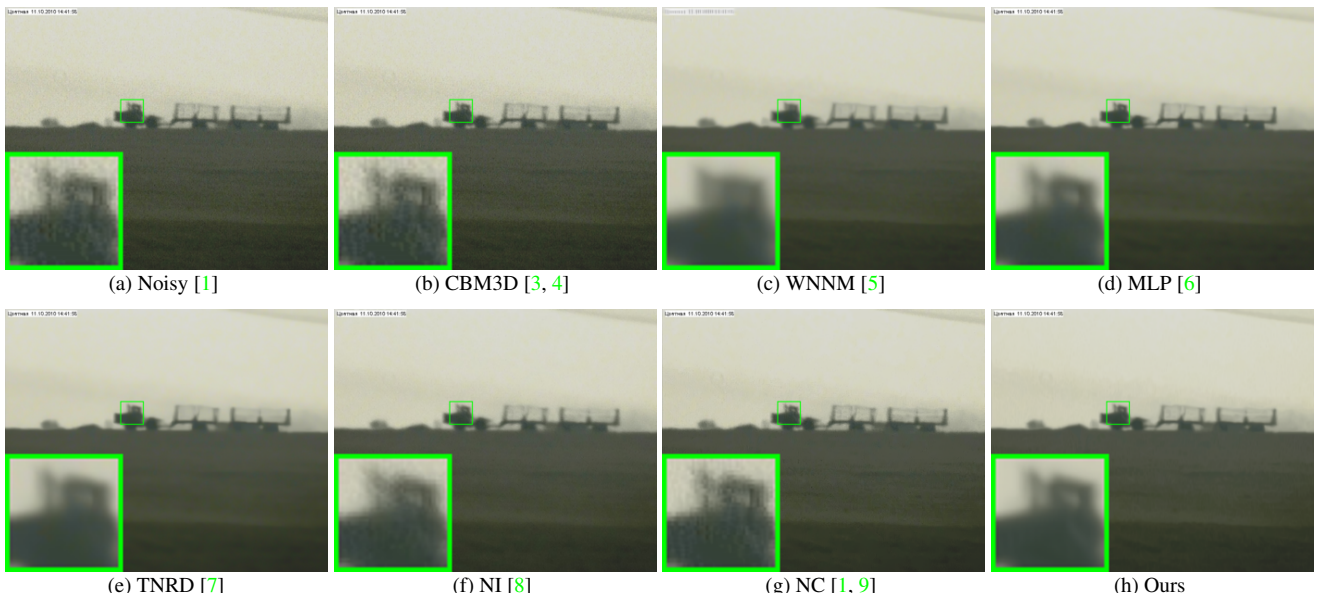
265

266

267

268

269

270  
271  
272  
273  
274  
275  
276  
277  
278  
279  
280  
281  
282  
283  
284  
285  
286  
287  
288  
289  
290  
291  
292  
293

(a) Noisy [1] (b) CBM3D [3, 4] (c) WNNM [5] (d) MLP [6]

(e) TNRD [7] (f) NI [8] (g) NC [1, 9] (h) Ours

Figure 4. Denoised images of the real noisy image “Vehicle” [1] by different methods. The images are better to be zoomed in on screen.

313

314

315

316

317

318

319

320

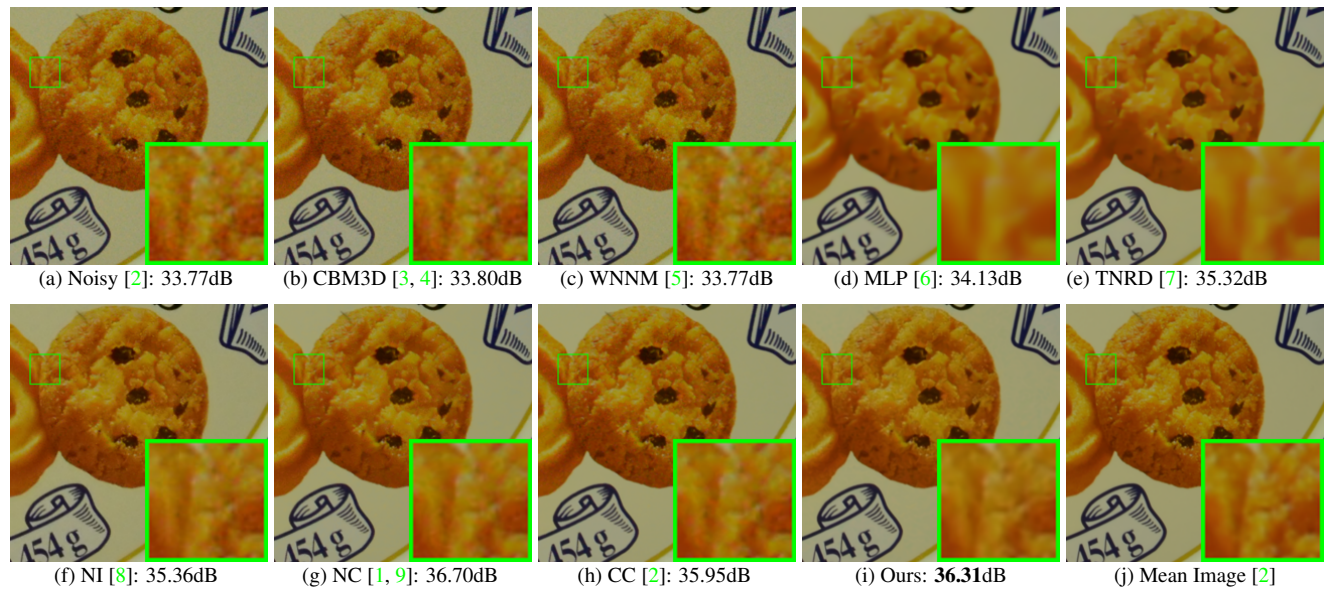
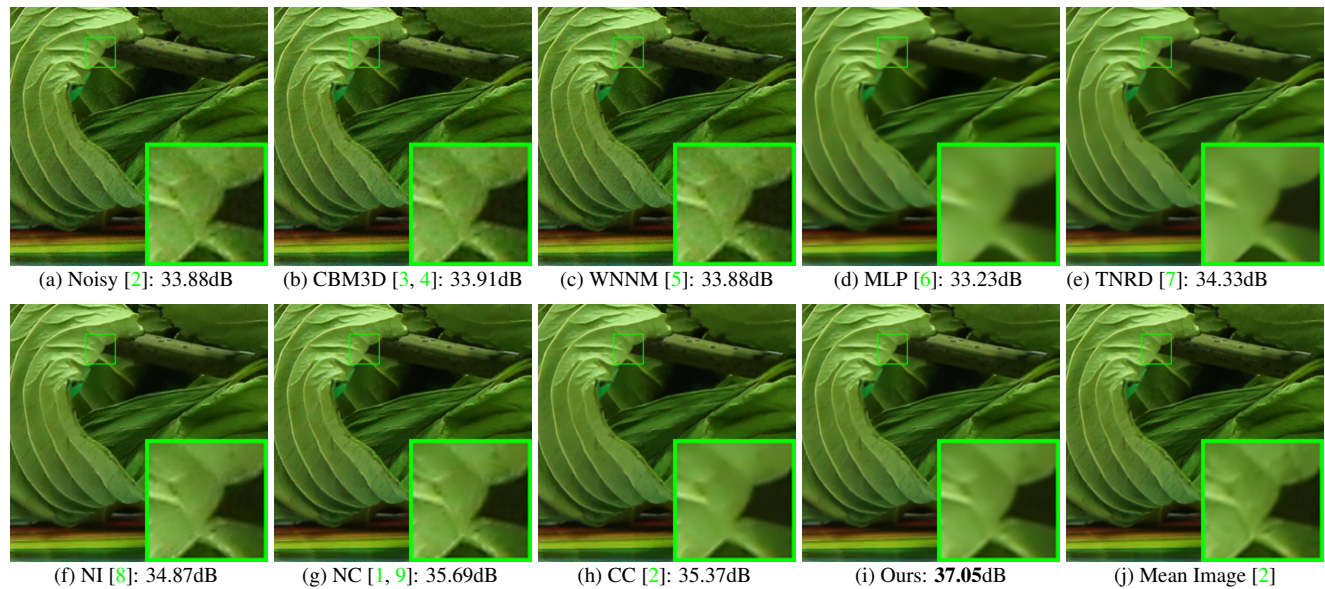
321

322

323

324 3. More Results on the 15 Cropped Images in [2] 378  
325 379

326 In this section, we provide more visual comparisons of the proposed method with the state-of-the-art denoising methods  
 327 on the 15 cropped real noisy images used in [2]. As can be seen from Figures 5-??, on most cases, our proposed method  
 328 achieves better performance than the competing methods. This validates the effectiveness of our proposed external prior  
 329 guided internal prior learning framework for real noisy image denoising.  
 330



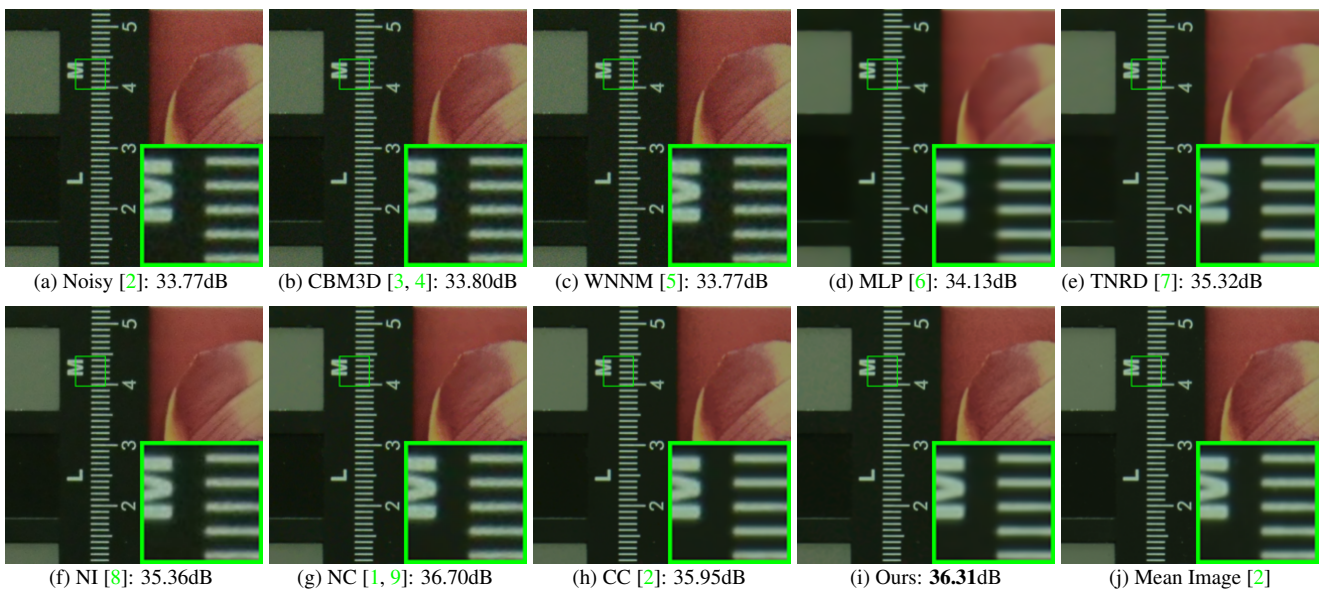


Figure 7. Denoised images of a region cropped from the real noisy image “Nikon D800 ISO 1600 2” [2] by different methods. The images are better to be zoomed in on screen.

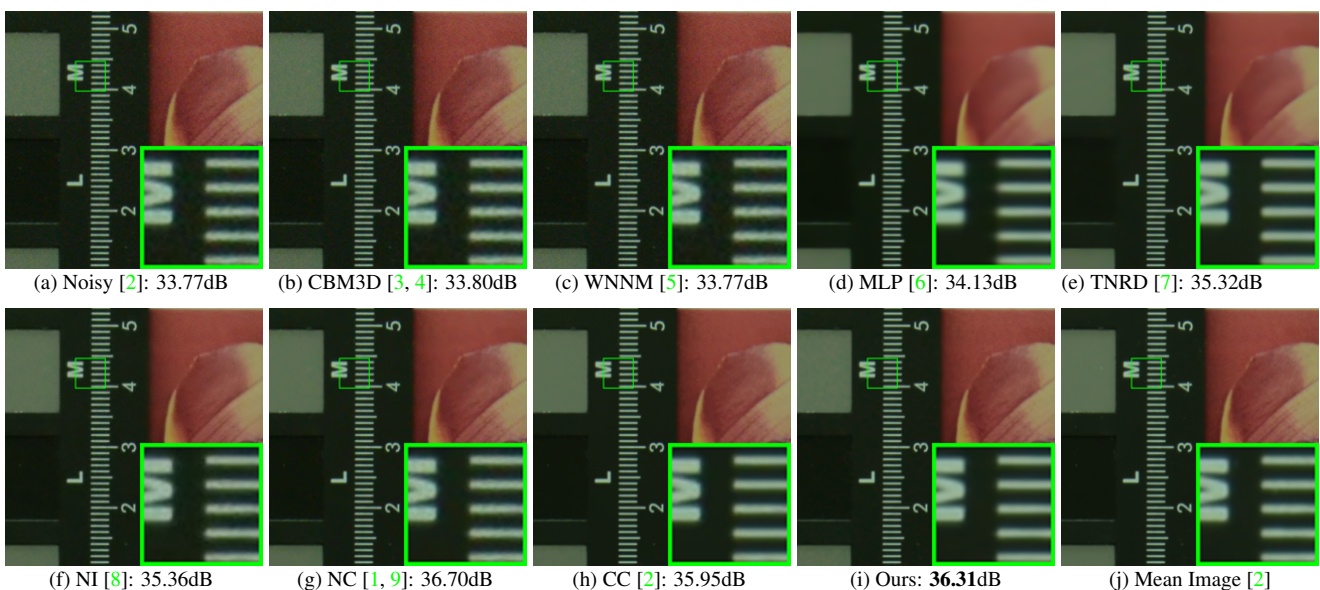


Figure 8. Denoised images of a region cropped from the real noisy image “Nikon D800 ISO 1600 2” [2] by different methods. The images are better to be zoomed in on screen.

## References

- [1] M. Lebrun, M. Colom, and J. M. Morel. The noise clinic: a blind image denoising algorithm. <http://www.ipol.im/pub/art/2015/125/>. Accessed 01 28, 2015. [1](#), [2](#), [3](#), [4](#), [5](#)
- [2] S. Nam, Y. Hwang, Y. Matsushita, and S. J. Kim. A holistic approach to cross-channel image noise modeling and its application to image denoising. *IEEE Conference on Computer Vision and Pattern Recognition (CVPR)*, pages 1683–1691, 2016. [1](#), [4](#), [5](#)
- [3] K. Dabov, A. Foi, V. Katkovnik, and K. Egiazarian. Image denoising by sparse 3-D transform-domain collaborative filtering. *IEEE Transactions on Image Processing*, 16(8):2080–2095, 2007. [2](#), [3](#), [4](#), [5](#)

- 540 [4] K. Dabov, A. Foi, V. Katkovnik, and K. Egiazarian. Color image denoising via sparse 3D collaborative filtering with grouping  
541 constraint in luminance-chrominance space. *IEEE International Conference on Image Processing (ICIP)*, pages 313–316, 2007. 2, 3,  
542 4, 5 594  
543 [5] S. Gu, L. Zhang, W. Zuo, and X. Feng. Weighted nuclear norm minimization with application to image denoising. *IEEE Conference*  
544 *on Computer Vision and Pattern Recognition (CVPR)*, pages 2862–2869, 2014. 2, 3, 4, 5 595  
545 [6] H. C. Burger, C. J. Schuler, and S. Harmeling. Image denoising: Can plain neural networks compete with BM3D? *IEEE Conference*  
546 *on Computer Vision and Pattern Recognition (CVPR)*, pages 2392–2399, 2012. 2, 3, 4, 5 596  
547 [7] Y. Chen, W. Yu, and T. Pock. On learning optimized reaction diffusion processes for effective image restoration. *IEEE Conference on*  
548 *Computer Vision and Pattern Recognition (CVPR)*, pages 5261–5269, 2015. 2, 3, 4, 5 597  
549 [8] Neatlab ABSoft. Neat Image. <https://ni.neatvideo.com/home>. 2, 3, 4, 5 598  
550 [9] M. Lebrun, M. Colom, and J.-M. Morel. Multiscale image blind denoising. *IEEE Transactions on Image Processing*, 24(10):3149–  
551 3161, 2015. 2, 3, 4, 5 599  
552 600  
553 601  
554 602  
555 603  
556 604  
557 605  
558 606  
559 607  
560 608  
561 609  
562 610  
563 611  
564 612  
565 613  
566 614  
567 615  
568 616  
569 617  
570 618  
571 619  
572 620  
573 621  
574 622  
575 623  
576 624  
577 625  
578 626  
579 627  
580 628  
581 629  
582 630  
583 631  
584 632  
585 633  
586 634  
587 635  
588 636  
589 637  
590 638  
591 639  
592 640  
593 641  
642  
643  
644  
645  
646  
647